Received: 24 February 2022 | Revised: 15 June 2022 | Accepted: 27 June 2022

DOI: 10.1002/hbm.26011

RESEARCH ARTICLE

WILEY

Different functional connectivity optimal frequency in autism compared with healthy controls and the relationship with social communication deficits: Evidence from gene expression and behavior symptom analyses

Jinjin Long[1,7] | Fengmei Lu[2] | Shanshan Yang[1] | Qianyue Zhang[1] | Xue Chen[1] | Yajing Pang[3] | Min Wang[4] | Bifang He[1] | Heng Liu[5] | Xujun Duan[2] | Huafu Chen[2] | Shaobing Ye[6] | Heng Chen[1,2]

[1]School of Medicine, Guizhou University, Guiyang, China

[2]Key laboratory for NeuroInformation of Ministry of Education, School of Life Science and Technology and Center for Information in BioMedicine, University of Electronic Science and Technology of China, Chengdu, China

[3]School of Electrical Engineering, Zhengzhou University, Zhengzhou, China

[4]Bioinformatics and BioMedical Bigdata Mining Laboratory, School of Big Health, Guizhou Medical University, China

[5]Department of Radiology, Affiliated Hospital of Zunyi Medical University, Medical Imaging Center of Guizhou Province, Zunyi, China

[6]The People's Hospital of Kaizhou District, Chongqing, China

[7]Guiyang Hospital of Stomatology, Guiyang, China

Correspondence
Huafu Chen, Key laboratory for NeuroInformation of Ministry of Education, School of Life Science and Technology and Center for Information in BioMedicine, University of Electronic Science and Technology of China, Chengdu, China.
Email: chenhf@uestc.edu.cn

Shaobing Ye, The People's Hospital of Kaizhou District, Chongqing, China.
Email: 825779777@qq.com

Heng Chen, School of Medicine, Guizhou University, Guizhou, China.
Email: hchen13@gzu.edu.cn

Funding information
Foundation Research Funds for Central Universities, Grant/Award Number: ZYGX2019Z017; Key Scientific Research Program of the Higher Education Institutions of Henan Province, Grant/Award Number: 22A416013; Key Technologies Research and Development Program of Henan Province, Grant/Award Number: 222102210076; Guizhou Provincial Science and Technology Projects, Grant/Award Numbers: [2020] 1Y407), [2020]1Y345, [2022]–general-038; National Natural Science Foundation of China,

Abstract

Studies have reported that different brain regions/connections possess distinct frequency properties, which are related to brain function. Previous studies have proposed altered brain activity frequency and frequency-specific functional connectivity (FC) patterns in autism spectrum disorder (ASD), implying the varied dominant frequency of FC in ASD. However, the difference of the dominant frequency of FC between ASD and healthy controls (HCs) remains unclear. In the present study, the dominant frequency of FC was measured by FC optimal frequency, which was defined as the intermediate of the frequency bin at which the FC strength could reach the maximum. A multivariate pattern analysis was conducted to determine whether the FC optimal frequency in ASD differs from that in HCs. Partial least squares regression (PLSR) and enrichment analyses were conducted to determine the relationship between the FC optimal frequency difference of ASD/HCs and cortical gene expression. PLSR analyses were also performed to explore the relationship between FC optimal frequency and the clinical symptoms of ASD. Results showed a significant difference of FC optimal frequency between ASD and HCs. Some genes whose cortical expression patterns are related to the FC optimal frequency difference of ASD/HCs were enriched for social communication problems. Meanwhile, the FC optimal frequency in ASD was significantly related to social communication

Grant/Award Numbers: 32060198, 62103377, 81871432, 62071099, 61901130, 61901129, U1808204

symptoms. These results may help us understand the neuro-mechanism of the social communication deficits in ASD.

KEYWORDS
autism spectrum disorder, optimal frequency, resting-state fMRI, social communication

1 | INTRODUCTION

Autism spectrum disorder (ASD) is a kind of neurodevelopmental disorder that is related with atypical brain function; it is primarily characterized by severely deficient social and communication ability and stereotyped behavior (Alexander-Bloch et al., 2013). In 2020, the estimated prevalence of ASD among American children was 1/54 (Maenner et al., 2020). The symptoms of ASD are related to the atypical functional communications across brain regions. Using resting-state functional magnetic resonance imaging (fMRI), several studies have explored the FC networks in ASD. In particular, atypical FCs of the triple network consisting of the salience network, central executive network, and default mode network (DMN) were frequently reported (Chen et al., 2017; Menon, 2011; Menon, 2019; Walsh et al., 2019; Yerys et al., 2015).

Human brain regions/connections have different frequency properties. Electroencephalogram (EEG) studies suggested that the human brain neuron activities are frequency-specific and associated with different human brain functions. The theta band (4–8 Hz) is related to memory, whereas alpha band (8–14 Hz) cognition (Herweg et al., 2020; Klimesch, 1999), beta band (14–30 Hz) motor control (Jurkiewicz et al., 2006), and gamma band (30–70 Hz) synchronization play a core role in cognition (Fries et al., 2008). The communication through coherence hypothesis suggests that information is transmitted between brain regions through oscillation phase synchronization at a specific frequency (Fries, 2015). Previous studies have reported the frequency specificity of the FC network in the human brain and the different spatial distributions of FC across different frequency bands. The insula, amygdala, and primary auditory cortex showed high connectivity in the >0.08 Hz frequency band, whereas the frontal lobe showed high connectivity in the <0.08 Hz frequency band (Salvador et al., 2008). The FC of three cortical networks, namely, sensorimotor, default mode, and visual, is most apparent at the 0.01–0.06 Hz frequency band, whereas that in limbic system regions is distributed over a wide frequency range (0.01–0.14 Hz) (Wu et al., 2008). These studies showed the existence of dominant frequency of brain connections.

Previous studies have reported that alteration of brain activity and FC in ASD were related to frequency. Gregory and coworkers found that the posterior dominant EEG rhythm in ASD was higher than that in controls, and the difference was more pronounced in the children subgroup (Gregory & Mandelbaum, 2012). Chen and coworkers constructed FC networks under Slow-4 (0.027–0.073 Hz) and Slow-5 (0.01–0.027 Hz) frequency bands to classify ASD and HCs. The results showed that the classification performance of the model trained with the FC of two frequency bands was better than that of the models trained with a single frequency band and low-frequency band (0.01–0.08 Hz); moreover, the classification scores between the cingulo-opercular network (CON) and DMN in Slow-4 were correlated with ASD symptom severity (Chen, Duan, et al., 2016). Duan and coworkers reported different under-connectivity patterns across slow-3–5 frequency bands in ASD, and the decreased connectivity of the Slow-3 band was significantly associated with the total and communication scores of autism diagnostic observation scale (ADOS) (Duan et al., 2017). Both studies have reported atypical FC patterns of ASD were frequency-specific and related with ASD behavior. These results might imply the alteration of the dominant frequency of FC in ASD. However, the atypical pattern of the dominant frequency of FC in ASD is still unclear.

In the present study, we aimed to explore the difference of the dominant frequency of FC between ASD and HCs by using an FC optimal frequency method. Then, we explored the relationship between the FC optimal frequency patterns and the clinical symptoms in ASD. On the basis of studies showing different dominant frequencies of the brain (Gregory & Mandelbaum, 2012) and frequency-specific FC patterns in ASD compared with HCs (Chen, Duan, et al., 2016; Duan et al., 2017), we hypothesized that the dominant frequency of FC in ASD has changed and may be related to ASD symptoms.

2 | MATERIALS AND METHODS

2.1 | Explanations of technical terms

The explanations of technical terms are presented here to help readers understand the methods section.

FC optimal frequency: the intermediate of the frequency bin at which the functional connection strength could reach the maximum.

FC optimal frequency strength: the functional connection strength under optimal frequency, which is the strongest connection across 16 frequency bins.

2.2 | Subjects

All resting-state fMRI images were obtained from the Autism Brain Imaging Data Exchange open-access database (ABIDE, https://fcon_1000.projects.nitrc.org/indi/abide/) (di Martino et al., 2014, 2017). The following inclusion criteria and final dataset were the same as those in a previous study (Duan et al., 2017): (1) Male subjects;

TABLE 1 Demographics of the subjects

	ASD	HCs	*p* value
Count	105	102	-
Age (years mean ± SD)	10.15 ± 1.26	10.02 ± 1.38	.48[a]
Handedness (R/L/mix)	83/9/13	82/5/15	.54[b]
Full scale IQ (mean ± SD)	110.53 ± 17.42	113.78 ± 11.98	.12[a]
Mean FD (mm mean ± SD)	0.17 ± 0.08	0.16 ± 0.08	.16[a]
Subject number from each site	16/14/34/14/11/16	15/14/34/14/11/14	.90[a]
Eye status (open/closed)	91/14	88/14	.93[b]
ADOS Gotham scores			
Social affect (mean ± SD)	8.91 ± 3.35	-	-
RRB (mean ± SD)	3.02 ± 1.84	-	-
Total (mean ± SD)	11.92 ± 4.06	-	-
Severity (mean ± SD)	6.89 ± 1.86	-	-

Abbreviations: ADOS Gotham scores, standardized scores of ADOS using Gotham algorithm, which has an improved prediction capacity for ASD; HCs, healthy controls; Mean FD, mean framewise displacement.
[a]Two-sample T-test.
[b]Chi-square test.

(2) Studies have shown that the abnormal brain function in ASD is highly related to age and tends to onset early (Lee et al., 2017; Long et al., 2016). Child period is critical as it is near the onset age and could avoid some environment confounding factors. Therefore, only child subjects aged 7–12 years were included in the present study; (3) Subjects with information of full-scale IQ, handedness, and eye status values; (4) Low head motion (lower than 2 mm translation, 2° rotation, the framewise displacement [FD] was used to assess head motion and less than 50% frames with FD above 0.5 mm) (Pang et al., 2022; Power et al., 2012); (5) Scan with complete cortical coverage; (6) A data-driven method was applied to subjects within each site to maximize the *p* values of group difference on age, full-scale IQ, handedness, eye status, and mean FD (Duan et al., 2017). For each step, we excluded one subject, with which the *p* values could increase the most. This step was repeated until the *p* values could not increase by excluding any subject; and (7) Sites with less than 10 subjects per group were excluded. Finally, 105 children with ASD and 102 HCs from six sites were included in this study. The detailed demographics of the subjects are shown in Table 1. The ABIDE id of each subject is shown in the Subject ID file.

2.3 | Image preprocessing

All resting-state fMRI data were preprocessed using the DPABI toolbox version 4.3 (http://rfmri.org/dpabi). The preprocessing steps were as follows. (1) Exclude the first 10 volumes of each subject. (2) Perform slice-timing and spatial head motion realign to correct the remaining volumes. (3) Despike via 3Ddespike in the AFNI toolbox (https://afni.nimh.nih.gov/afni/). The Despike step could remove the potential motion artifacts in resting-state fMRI data and retain continuous temporal information of signals. (4) Remove the linear trends. (5) Normalize resting-state fMRI maps to the standard MNI space by using EPI template. (6) Regress the noise signals, including 24 head motion parameters and mean signals of white matter and cerebrospinal fluid. (7) Smooth with Gaussian kernel of 6-mm full width at half maximum. (8) Filter 16 times. Of note, the TR has a maximum of 3 s, and the frequency interval is set to 0.01. Therefore, 16 frequency bins (0.01–0.17 Hz) were used in this study.

2.4 | Site-specific effect

Given that the fMRI dataset came from multiple sites, the results might rely on a specific site and be affected by site difference. We selected the site that have more than 10 samples to maintain data balance between sites and verified that there was no difference in site composition between ASD and HCs by chi-square test ($p = .90$). Then, we performed the regression on each FC network with the site as a covariant using the dummy coding scheme. One-way ANOVA was conducted on the FC optimal frequency of high-weight FCs of all subjects across sites to determine whether the site difference affects the results. The maximum *p* value was 1, and the minimum was 0.5 (FDR corrected), which indicated that the site difference has little influence on the FC optimal frequency. The site scan parameters are shown in Table S2.

2.5 | FC optimal frequency

A total of 160 coordinates were used to define the regions of interest (ROIs) across the brain in a previous study (Dosenbach et al., 2010).

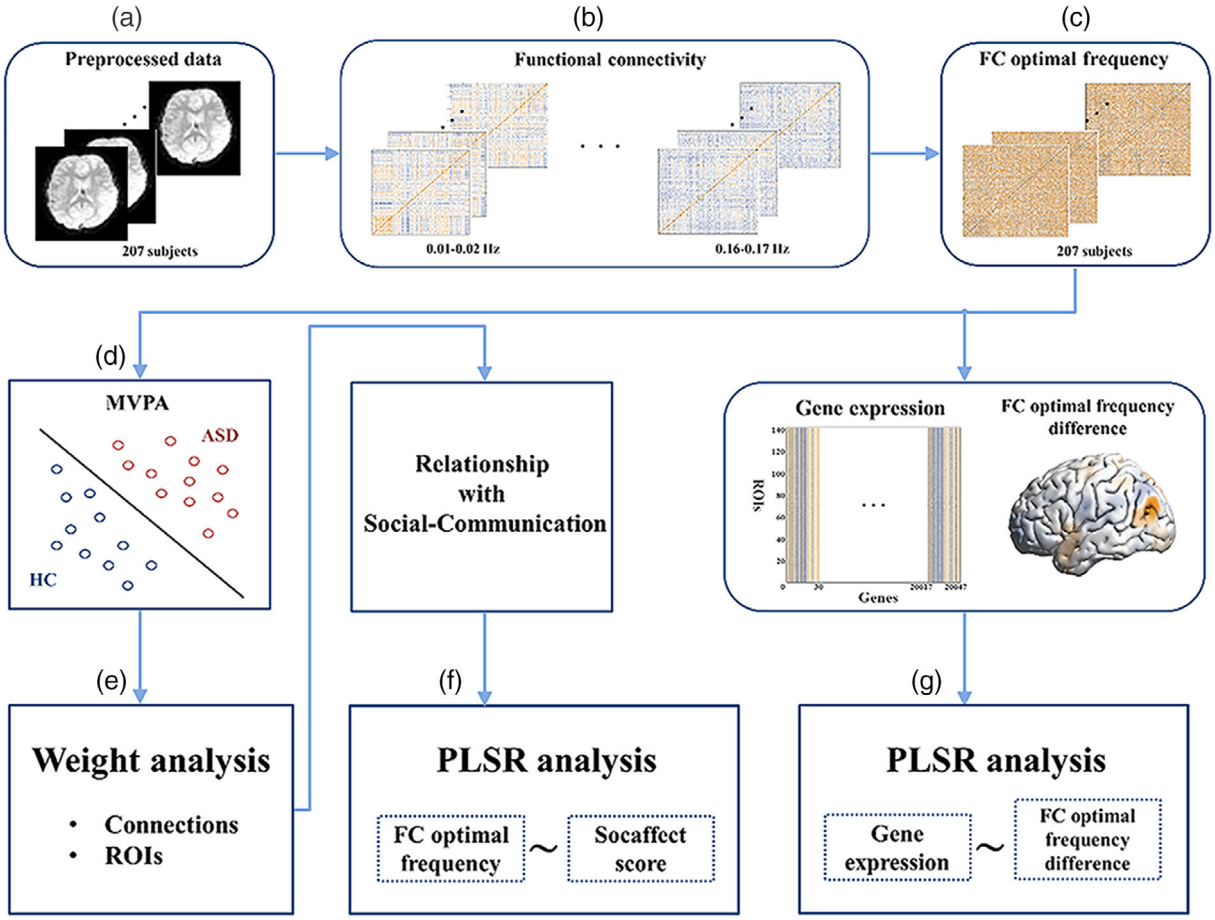

FIGURE 1 Flowchart of FC optimal frequency analyses. (a) Preprocessed resting-state functional magnetic resonance imaging (rs-fMRI) data of 105 autism spectrum disorder (ASD) and 102 healthy controls (HCs). (b) Calculate the functional connectivity (FC) network across 16 frequency bins, and each connection has 16 connection strengths. (c) Calculate the intermediate of the frequency bin that has the maximum FC strength, which is called the FC optimal frequency. (d) The FC optimal frequency was used as the feature of the linear support vector machine (SVM) to distinguish ASD from HCs. (e) Weight analyses were conducted to identify high-weight FCs and brain regions, which indicate significantly different FC optimal frequency between ASD and HCs. (f) Partial least squares regression (PLSR) analysis was conducted to explore the relationship between optimal frequency of high-weight FCs and social affect score of ASD. (g) PLSR analysis was conducted to explore the relationship between cortical gene expression and FC optimal frequency difference of ASD/HCs.

These brain ROIs were divided into six networks, including sensorimotor network (SMN), CON, DMN, fronto-parietal network (FPN), occipital network (ON) and cerebellum network (CN). In the present study, CN was excluded because the primarily focus was on cortical networks. Therefore, the remaining 142 coordinates were used to create 5-mm-radius spherical ROIs, which represent the network nodes.

The averaged fMRI signals in the 142 ROIs were extracted and band-pass filtered using the 16 predefined frequency bins (0.01–0.02, 0.02–0.03, ..., 0.16–0.17 Hz). Then, the Pearson correlation coefficient was calculated to determine the FC between pairwise ROIs, and 16 FC networks were constructed across 16 frequency bins. For each connection, 16 FC strengths were obtained across 16 different frequency bins. The FC optimal frequency was defined as the intermediate value of the frequency band at which the FC strength could reach the maximum. The FC optimal frequency was used to measure the dominant frequency of FC. Therefore, a 142 × 142 FC optimal frequency network was obtained for each subject (Figure 1).

2.6 | Multivariate pattern analysis of the FC optimal frequency

Multivariate pattern analysis (MVPA) was applied to the FC optimal frequency network of each subject to assess whether the FC optimal frequency in ASD is significantly different from that of HCs. The analysis course was the same as that in a previous study (Chen, Duan, et al., 2016). Here, the FC optimal frequency between ROIs was used as the classification feature. As the number of features is greater than the number of subjects, "overfitting" may occur. Therefore, the F-score method was applied for feature selection to obtain the most important features, and features with a larger F-score were more likely to have potential to discriminate ASD from HCs. A range of feature numbers were utilized because the optimal feature number was unknown. The model construction and evaluation were performed at a computational server (Sugon I840-G20; Dawning Information Industry Co., LTD., Beijing, China).

Support vector machine (SVM) classifier works well in cases with small sample size and large feature size. As a type of supervised learning, SVM constructs the decision function from the training dataset and labels (ASD or HCs). Then the model could predict the class labels of the test dataset. In the present study, a linear kernel was used because it could reduce the risk of overfitting (Pereira et al., 2009). The LIBLINEAR toolbox (Fan et al., 2008) with default parameters was utilized to conduct SVM classification. The leave-one-out cross-validation (LOOCV) strategy was used to calculate the accuracy, sensitivity, and specificity to evaluate the classification performance.

Following MVPA, a permutation test with 1000 trials was performed to determine whether the accuracy was significantly higher than random cases. In each trial, the labels of all subjects were shuffled, and then MVPA was applied to the original features and shuffled labels. This procedure was the same as the MVPA on the original dataset. The permutation p value was calculated by the number of trials, whose accuracy was higher than that based on the original dataset. As a comparison, MVPA was also applied to the FC optimal frequency strength of each subject to determine whether the FC optimal frequency strength is different between ASD and HCs.

2.7 | Optimal frequency weight analyses

The classification weights for all FCs were calculated to determine the importance level of each connection in the classification model. The classification weights could be obtained for each trial of LOOCV. The classification weight of each connection was calculated by averaging the absolute values of classification weights across all LOOCV trials, and the weights of connections that were not included in the classification model were set as zero (Chen, Duan, et al., 2016; Liu et al., 2015). Connections with classification weight above mean ± SD across all connections were considered as high-weight FCs. For each ROI, the classification weight was then calculated by summing up the classification weights of the high-weight FCs associated with the ROI.

2.8 | Relationship between the FC optimal frequency difference of ASD/HCs and cortical gene expression

ASD is known to have strong genetic underpinnings. PLSR analysis was conducted to explore the relationship between the FC optimal frequency difference of ASD/HCs and the genotype (Li et al., 2021; Romero-Garcia et al., 2019). The optimal frequency of each ROI for each subject was defined as the mean optimal frequency of the connections that connect the ROI, and we calculated it across subjects in the ASD and HC groups. The FC optimal frequency difference levels of each ROIs in ASD/HCs were defined as the mean optimal frequency in ASD minus the one in HCs. The brain-wide gene expression data came from the Allen Institute for Brain Science (AIBS) dataset, which were measured in six postmortem brains of 3702 spatially distinct samples. Each sample's MNI coordinate and the expression values of 20,647 genes were also provided. As the gene expression values were from six different postmortem brains, the gene expression values were first z-transformed. For each brain ROI in the Dosenbach atlas, the gene expression values were linearly interpolated by the six nearest samples of the AIBS dataset (Hawrylycz et al., 2015). Then, 20,647 regional gene expression values were obtained for each brain ROI. The PLSR method was used to identify which genes were significantly associated with the FC optimal frequency difference of ASD/HCs. The PLSR component number was set as 35, which is the same as that in a previous study (Romero-Garcia et al., 2019). The PLSR component with the most explanatory contribution was considered significant. For the significant component, the PLSR weights of 20,647 genes were z-transformed based on one-tail Z distribution (Li et al., 2021), and genes with $p < .05$ (FDR corrected) were considered to have significant association with the FC optimal frequency difference of ASD/HCs. Enrichment analysis was utilized to determine the function of the significant genes. The Kobas toolbox (http://kobas.cbi.pku.edu.cn/kobas3) was used, and the result with $p < .05$ (FDR corrected) was retained (Bu et al., 2021).

2.9 | Relationship between FC optimal frequency and clinical symptoms of ASD

PLSR analyses were also conducted to further determine the relationship between the FC optimal frequency and the clinical symptoms in ASD. Similar to the cortical gene expression analysis, the PLSR component number was set as 35 and the one with the largest explanatory power was used to calculate the Pearson correlation coefficient with the ADOS Gotham diagnostic score. Statistical significance was considered at $p < .05$ (FDR corrected). Here, the ADOS Gotham social affect score, ADOS Gotham RRB score, and ADOS Gotham diagnostic score were included in the PLSR analysis. The social affect score is a standardized score of ADOS raw score, which combines the ADOS social score and communication score (Dorlack et al., 2018; Gotham et al., 2007). The RRB score is the restricted and repetitive behavior total subscore, and the severity score is the individually calibrated severity subscore. The ADOS Gotham diagnostic score measures the symptoms of ASD that adjusted the effect of age and verbal levels (Gotham et al., 2007).

3 | RESULTS

3.1 | MVPA results

MVPA revealed a difference in the FC optimal frequency between ASD and HCs (accuracy = 72.95%, permutation $p < .001$). By comparison, we applied the same model to the FC optimal frequency strength, and the result showed a significant ability to classify ASD and HCs (accuracy = 62.8%, permutation $p = .003$). However, the accuracy was much lower than the one based on the FC optimal frequency, which revealed that the FC optimal frequency difference

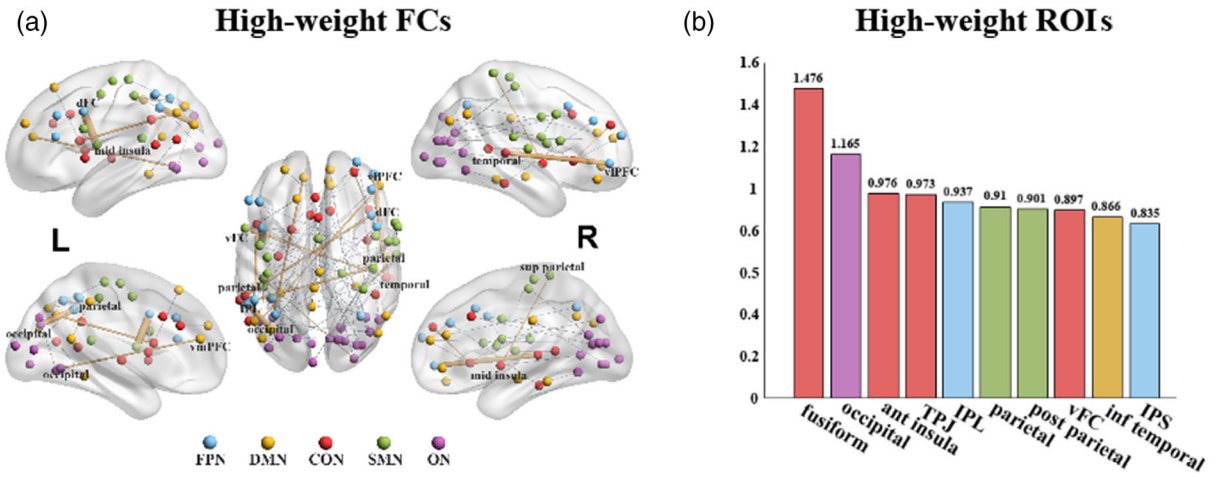

(c) **High-weight FCs distribution**

Subnetworks	FPN		DMN		CON		SMN		ON	
Difference	ASD>HC	ASD<HC	ASD>HC	ASD<HC	ASD>HC	ASD<HC	ASD>HC	ASD<HC	ASD>HC	ASD<HC
	Weight(%)		Weight(%)		Weight(%)		Weight(%)		Weight(%)	
FPN	0.52 (1.26%)									
DMN	1.09 (2.65%)	0.6 (1.47%)	1.34 (3.26%)							
CON	5.52 (13.4%)		2.83 (6.88%)	0.75 (1.83%)	2.06 (5%)					
SMN	1.64 (3.98%)		1.78 (4.33%)	1.53 (3.71%)	3.19 (7.76%)	0.65 (1.58%)	1.7 (4.12%)	1 (2.4%)		
ON	1.43 (3.46%)	1.59 (3.86%)	4.38 (10.63%)		2.97 (7.21%)	0.6 (1.45%)	1.18 (2.86%)	2.26 (5.48%)	0.59 (1.43%)	
Total	10.2 (13.57%)	2.19 (2.91%)	11.42 (15.19%)	2.88 (3.83%)	16.57 (22.04%)	2 (2.66%)	9.49 (12.62%)	5.44 (7.24%)	10.55 (14.03%)	4.45 (5.92%)

FIGURE 2 Multivariate pattern analysis (MVPA) results. (a) Sixty-eight high-weight functional connectivities (FCs). The bold connections are the top 10. (b) Top 10 among 83 high-weight ROIs. (c) High-weight FCs between brain networks (including fronto-parietal network [FPN], default mode network [DMN], cingulo-opercular network [CON], sensorimotor network [SMN], and occipital network [ON]). The number of each network connection represents the sum of the weights of high-weight FCs, and the percentage represents the proportion of the weight in all high-weight FCs. The number in the total line represents the network weight, which is the sum of the weights of high-weight FCs in the network, and the percentage represents the proportion of the weight in all network weights (yellow indicates autism spectrum disorder [ASD] with higher FC optimal frequency than healthy controls [HCs], and blue indicates ASD with lower FC optimal frequency than HCs).

between ASD and HCs was more pronounced than the FC optimal frequency strength. The distribution and the MVPA results based on the FC optimal frequency strength are shown in Figure S3-S4.

Weight analyses showed that the FCs between CON and FPN have the highest classification weight. Compared with HCs, most of the high-weight FCs showed higher optimal frequency. The FC optimal frequency of ASD was concentrated between 0.08 and 0.11 Hz, whereas that of HCs was between 0.07 and 0.09 Hz (the distribution of FC optimal frequency is shown in Figure S2). The ROIs with high classification weight were more located at the CON, including fusiform, ant insula, temporoparietal junction (TPJ), and ventromedial frontal cortex (vFC). For visualization, only the top 10 regions with the highest classification weight are shown in Figure 2b.

3.2 | Gene PLSR analysis and enrichment

A total of 35 PLSR gene components were obtained according to PLSR analysis. The explanatory power of the PLSR1 gene component reached 22.84%. The correlation coefficient between the FC optimal frequency difference of ASD/HCs and the score of PLSR1 gene component was 0.478 (p < 10e-7, FDR corrected, Figure 3a). In the PLSR1 gene component, 61 genes showed significantly higher weights than others (p < .05, FDR corrected). Then, enrichment analysis identified genes that were enriched for "social communication problems" (p = .025, FDR corrected), including *XIRP1* and *IRX5*. Genes with high PLSR weights included *OR13C4*, *RGR*, and *C19orf21*. Sixty-one genes after FDR correction are listed in Figure S5.

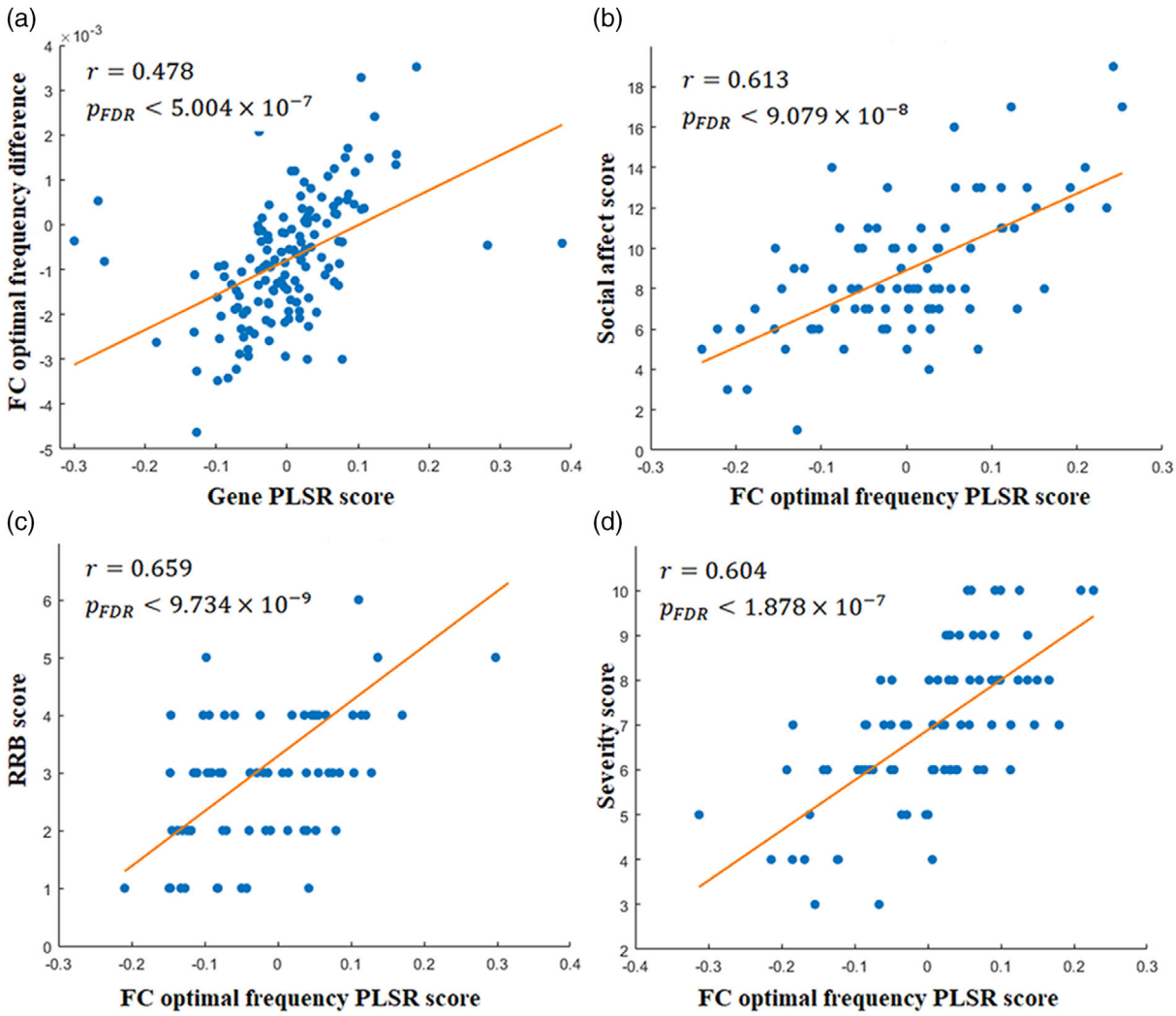

FIGURE 3 Partial least squares regression (PLSR) results. (a) Relationship between the functional connectivity (FC) optimal frequency difference of autism spectrum disorder/healthy controls (ASD/HCs) and cortical gene expression. (b) Relationship between social affect and FC optimal frequency. (c) Relationship between restricted and repetitive behaviors and FC optimal frequency. (d) Relationship between severity and FC optimal frequency

3.3 | Correlation between FC optimal frequency and clinical symptoms of ASD

A total of 68 connections with high classification weight in MVPA were found in this study. As shown in Figure 3, the FC optimal frequency of high-weight connections showed significant correlation with ADOS Gotham social affect score ($r = .613$, $p < 10e\text{-}8$), ADOS Gotham RRB score ($r = .659$, $p < 10e\text{-}9$), and ADOS Gotham diagnostic score ($r = .604$, $p < 10e\text{-}7$). All p values were FDR corrected.

3.4 | FC optimal frequency distribution in HCs

We explored the optimal frequency of all FCs in the HCs group. The results showed that the mean FC optimal frequency was 0.0894 Hz, ranging from 0.074 to 0.1067 Hz. At the subnetwork level, the FC optimal frequency did not show much difference between each subnetwork (shown in Figure S6). At the connection level, connections with high FC optimal frequency mainly concentrated in ON-SMN, ON-FPN, and SMN-DMN, and connections with low FC optimal frequency mainly concentrated in ON-DMN (shown in Figure S7).

4 | DISCUSSION

4.1 | Analytic overview

This study revealed the significant differences in the FC optimal frequency between ASD and HCs. In addition, the FC optimal frequency strength showed poor ability to distinguish ASD and HCs. The results implied that for some connections in ASD, the functional information transmission between brain regions may not be simply damaged but

shift from the original optimal frequency to other frequencies. The enrichment analysis showed that the FC optimal frequency difference between the two groups was related to social communication problems. The FC optimal frequency in ASD was associated with behavioral symptoms, which include social affect, RRB, and severity. These results may help us understand the atypical neuro information transmission pattern and provide a novel neuro-marker to evaluate the social-communication severity level of ASD.

4.2 | FC optimal frequency difference between ASD and HCs

Previous FC studies have reported damaged functional information transmission between specific brain regions in ASD based on the whole low-frequency band rs-fMRI data (Chen, Uddin, et al., 2016; Hong et al., 2019). However, evidence suggested different frequency properties with different connections, and atypical FC patterns in ASD were frequency-specific (Chen, Duan, et al., 2016; Salvador et al., 2008; Wu et al., 2008).

The classification accuracy based on the FC optimal frequency achieved a relatively high accuracy (72.95%), but it is still lower than that in a previous study based on FC (accuracy = 79.17%) (Chen, Duan, et al., 2016). The reasons may be due to the differences in datasets and preprocessing and cross-validation methods. In the present study, we also constructed a classification model based on the FC optimal frequency strength (accuracy = 62.80%), which revealed that FC optimal frequency has greater discriminative potential than FC optimal frequency strength, and the FC optimal frequency of high-weight FCs in ASD showed higher frequency than HCs. Based on these results, we speculated that the lower FC frequently reported in ASD in the low-frequency range was due to the frequency specificity of FC rather than connection strength damage. Figure 2c illustrates that the optimal frequency of most high-weight FCs in ASD was higher than that in HCs, especially the connections between CON and FPN, which might imply that the co-activation between neurons of specific brain regions occurs at a higher frequency band in ASD. This finding suggests that the FC in ASD needs to be studied at a higher frequency range. The higher FC optimal frequency could be possibly related to the imbalanced excitation/inhibition of neural activity in ASD. Previous studies have reported excess of excitation and loss of inhibition in ASD brain (Nelson & Valakh, 2015). The excess of excitation may cause more frequent brain activity and induce the higher connection frequency in ASD.

4.3 | Relationships with social communication of ASD

The PLSR analysis between the FC optimal frequency of significant connections and the ADOS Gotham social affect score showed that the FC optimal frequency in ASD was associated with social and communication ability. As shown in Figure 2c, CON showed the highest ASD/HCs difference in the FC optimal frequency, and the connections between CON and FPN exhibited the most classification weight. CON becomes active whenever cognitive engagement is required, and it maintains tonic alertness (Sadaghiani & D'Esposito, 2015). A previous study suggested that the heightened salience of social and emotional information provides a flexible social response in adolescence (Rosen et al., 2018). The FPN and fronto-temporal network are considered to comprise the social brain, and FPN is involved in the process of social coordination and cognition (Burns, 2006; Dumas et al., 2020). Moreover, CON and FPN are part of the triple network system, and abnormalities in these regions have been reported in FC studies in ASD (Kleinhans et al., 2008; Perez Velazquez et al., 2009). The results of the present study suggested that the altered FC optimal frequency in these two networks may lead to atypical social information salience and processing and result in social deficits in ASD. The connections between CON and FPN, CON and SMN, and DMN and ON bore the highest classification weights. The abnormal FC optimal frequency between these networks supported that atypical FC patterns was concentrated in the salience, executive, visual, and default-mode networks in ASD (Raatikainen et al., 2020).

The FC optimal frequency difference between ASD and HCs was associate with *IRP1* and *IRX5*, genes identified by PLSR1 as enriched in social communication problems. These two genes are associated with the phenotype of social communication, suggesting that social communication abilities are heritable, and the genetic difference of that phenotype in ASD has been reported (St Pourcain et al., 2014). Our results revealed the relationship between social-communication-related genes and FC optimal frequency difference of ASD/HCs. Among the social-communication-related genes, *XIRP1* (or *Xin*α) codes Xin actin-binding repeat-containing protein that could protect actin filaments during depolymerization. A previous study showed impaired dynamics of actin polymerization in an ASD patient subgroup (Griesi-Oliveira et al., 2018). *IRX5* is involved in "cell development," "neuron differentiation," "response to stimulus," and "visual perception" processes of Gene Ontology terms (Gaudet et al., 2011). Although the two genes are related to social skills, they are only weak candidates for ASD susceptibility loci because they are poorly studied and should be further researched in the molecular genetics of ASD in the future. The *OR13C4* and *RGR* genes have high weight in gene PLSR analysis. The *OR13C4* gene enables olfactory receptor activity, a G protein-coupled receptor that conducts olfactory signals. Olfactory perception has been reported to play an important role in the regulation of human social behaviors (Sarafoleanu et al., 2009). A previous study also revealed that olfactory receptors in ASD were most associated with copy number variation (Schuch et al., 2019). The *RGR* gene encodes retinal G protein-coupled receptor, which is involved in visual perception. ASD showed abnormal visual behavior after 12 months (Ozonoff et al., 2008), and changed visual perception may make ASD unable to process complex social information, resulting in abnormal social behavior. These two genes may reveal that ASD has sensory system changes in the perception and transmission of social

information, and the pathogenic mechanism of social deficits in ASD may be explored by studying the genes/proteins related to sensation.

The present study showed the association between FC optimal frequency in ASD and the social communication problem via gene expression and behavioral symptom aspects. The results suggested that the ASD/HCs difference of FC optimal frequency may be due to physiological mechanisms regulated by relevant genes. It may lead to atypical FC of social function-related regions and ultimately influence the social development in ASD.

4.4 | Genetic explanations for the FC optimal frequency difference in ASD

The *C19orf21* and *ARHGAP6* genes were found in the PLSR analysis between the FC optimal frequency difference of ASD/HCs and gene expression. The *C19orf21* gene enables actin filament binding, and the *ARHGAP6* gene promotes actin remodeling. Both are involved in actin formation. Actin provides important support for neuronal development and synaptic plasticity and is involved in the important signaling pathway that is highly associated with mental diseases and neurodevelopmental disorders (Dent et al., 2011; Flynn, 2013; Yan et al., 2016). Synaptic plasticity adjusts the number and/or strength of synapses and alters the organization and activity of neural circuits, resulting in different functional network characteristics (Stampanoni Bassi et al., 2019; Vitureira et al., 2012). These results may reveal that the synaptic cytoskeleton changes in ASD lead to abnormal synaptic plasticity, which may be the underlying cause of the unbalanced excitation mechanism in the FC network in ASD.

4.5 | Broader correlation with symptoms of ASD

Previous studies have found that the frequency-specific FC was associated with social deficits and total symptoms in ASD (Duan et al., 2017). In the present study, our results not only showed consistent correlation, but indicated that the restricted interests/repetitive behaviors and severity of ASD were significantly correlated with FC optimal frequency. This provided further evidence that the FC optimal frequency was associated with ASD behaviors.

4.6 | FC optimal frequency in HCs

The traditional FC studies mainly concentrated on the low-frequency band (<0.1 Hz). However, we found that the FC optimal frequency of whole brain connections in HCs ranges from 0.074 to 0.1067 Hz (as shown in Figure S7), and the optimal frequency of some FCs is greater than 0.1 Hz. Therefore, we consider that the FC patterns in the high-frequency band are also important in resting-state FC studies, especially for visual/sensorimotor studies. Future studies based on larger samples are needed to assess the frequency bands for resting-state FC studies.

4.7 | Limitation

In PLSR analysis, a strong correlation between the FC optimal frequency difference of ASD/HCs and the cortical gene expression was found. However, the gene expression data were collected from six postmortem brains of adults, whereas the research subjects in the present study were children. Because gene expression changes with age, the gene expression results need to be considered with caution. Future studies may require a dataset with age-matched rs-fMRI and gene expression data (or both from the same subjects). In addition, our study only included male samples, which could not represent the whole community of children with ASD. Whether there is a general change or gender-specific effect in the FC optimal frequency in children with ASD needs further study. Given that brain dysfunction in ASD occurs during early brain development, we included children aged 7–12 years. The FC optimal frequency deference between ASD and HCs has been found in children, but the results cannot be generalized to all ages due to symptoms varying with age. Whether the FC optimal frequency has changed in older patients and its trajectory with age need further study.

5 | CONCLUSIONS

The study revealed that the optimal frequency of some resting-state FCs in ASD was higher than that in HCs. The gene expression and clinical symptom evidence showed that the FC optimal frequency difference of ASD/HCs is related to social communication deficits in ASD. The results imply an altered dominant frequency property of the neural transmission mechanism in ASD, which may provide a biomarker for behavioral symptoms of ASD, particularly of social communication deficits.

ACKNOWLEDGMENTS

The authors would like to thank the Autism Brain Image Data Exchange and Allen Institute for Brain Science for their support, they provided an open-access database and generously shared resting-state fMRI data.

FUNDING INFORMATION

The present study was supported by the National Natural Science Foundation of China (Nos. 61901129, 61901130, 62071099, 81871432, U1808204, 62103377, and 32060198), Guizhou Provincial Science and Technology Projects ([2022]–general-038, [2020] 1Y345, and [2020]1Y407), the Key Technologies Research and Development Program of Henan Province (222102210076), the Key Scientific Research Program of the Higher Education Institutions of Henan Province (22A416013), and the Foundation Research Funds for Central Universities (ZYGX2019Z017).

CONFLICT OF INTEREST

The authors declare that they have no competing interests.

DATA AVAILABILITY STATEMENT

All rs-fMRI data used in this study could be found at the ABIDE open-access dataset (https://fcon_1000.projects.nitrc.org/indi/abide/). Gene dataset was created by the Allen Institute for Brain Science (AIBS) (http://human.brain-map.org).

ORCID

Yajing Pang https://orcid.org/0000-0003-4070-6748
Bifang He https://orcid.org/0000-0002-9906-3794
Heng Liu https://orcid.org/0000-0002-6108-5154
Xujun Duan https://orcid.org/0000-0001-8543-2117
Huafu Chen https://orcid.org/0000-0002-4062-4753
Heng Chen https://orcid.org/0000-0001-6939-7665

REFERENCES

Alexander-Bloch, A., Raznahan, A., Bullmore, E., & Giedd, J. (2013). The convergence of maturational change and structural covariance in human cortical networks. *The Journal of Neuroscience*, *33*(7), 2889–2899.

Bu, D., Luo, H., Huo, P., Wang, Z., Zhang, S., He, Z., Wu, Y., Zhao, L., Liu, J., Guo, J., Fang, S., Cao, W., Yi, L., Zhao, Y., & Kong, L. (2021). KOBAS-i: Intelligent prioritization and exploratory visualization of biological functions for gene enrichment analysis, *49*, W317–W325. https://doi.org/10.1093/nar/gkab447

Burns, J. (2006). The social brain hypothesis of schizophrenia. *World Psychiatry*, *5*(2), 77–81.

Chen, H., Duan, X., Liu, F., Lu, F., Ma, X., Zhang, Y., Uddin, L. Q., & Chen, H. (2016). Multivariate classification of autism spectrum disorder using frequency-specific resting-state functional connectivity—A multi-center study. *Progress in Neuro-Psychopharmacology & Biological Psychiatry*, *64*, 1–9.

Chen, H., Uddin, L. Q., Duan, X., Zheng, J., Long, Z., Zhang, Y., Guo, X., Zhang, Y., Zhao, J., & Chen, H. (2017). Shared atypical default mode and salience network functional connectivity between autism and schizophrenia. *Autism Research*, *10*(11), 1776–1786.

Chen, H., Uddin, L. Q., Zhang, Y., Duan, X., & Chen, H. (2016). Atypical effective connectivity of thalamo-cortical circuits in autism spectrum disorder. *Autism Research*, *9*(11), 1183–1190.

Dent, E. W., Gupton, S. L., & Gertler, F. B. (2011). The growth cone cytoskeleton in axon outgrowth and guidance. *Cold Spring Harbor Perspectives in Biology*, *3*(3), a001800.

di Martino, A., O'Connor, D., Chen, B., Alaerts, K., Anderson, J. S., Assaf, M., Balsters, J. H., Baxter, L., Beggiato, A., Bernaerts, S., Blanken, L. M. E., Bookheimer, S. Y., Braden, B. B., Byrge, L., Castellanos, F. X., Dapretto, M., Delorme, R., Fair, D. A., Fishman, I., … Milham, M. P. (2017). Enhancing studies of the connectome in autism using the autism brain imaging data exchange II. *Scientific Data*, *4*, 170010.

di Martino, A., Yan, C. G., Li, Q., Denio, E., Castellanos, F. X., Alaerts, K., Anderson, J. S., Assaf, M., Bookheimer, S. Y., Dapretto, M., Deen, B., Delmonte, S., Dinstein, I., Ertl-Wagner, B., Fair, D. A., Gallagher, L., Kennedy, D. P., Keown, C. L., Keysers, C., … Milham, M. P. (2014). The autism brain imaging data exchange: Towards a large-scale evaluation of the intrinsic brain architecture in autism. *Molecular Psychiatry*, *19*(6), 659–667.

Dorlack, T. P., Myers, O. B., & Kodituwakku, P. W. (2018). A comparative analysis of the ADOS-G and ADOS-2 algorithms: Preliminary findings. *Journal of Autism and Developmental Disorders*, *48*(6), 2078–2089.

Dosenbach, N. U., Nardos, B., Cohen, A. L., Fair, D. A., Power, J. D., Church, J. A., Nelson, S. M., Wig, G. S., Vogel, A. C., Lessov-Schlaggar, C. N., Barnes, K. A., Dubis, J. W., Feczko, E., Coalson, R. S., Pruett, J. R., Jr., Barch, D. M., Petersen, S. E., & Schlaggar, B. L. (2010). Prediction of individual brain maturity using fMRI. *Science*, *329*(5997), 1358–1361.

Duan, X., Chen, H., He, C., Long, Z., Guo, X., Zhou, Y., Uddin, L. Q., & Chen, H. (2017). Resting-state functional under-connectivity within and between large-scale cortical networks across three low-frequency bands in adolescents with autism. *Progress in Neuro-Psychopharmacology & Biological Psychiatry*, *79*, 434–441.

Dumas, G., Moreau, Q., Tognoli, E., & Kelso, J. A. S. (2020). The human dynamic clamp reveals the fronto-parietal network linking real-time social coordination and cognition. *Cerebral Cortex*, *30*(5), 3271–3285.

Fan, R., Chang, K., Hsieh, C., Wang, X., & Lin, C. (2008). LIBLINEAR: A library for large linear classification. *Journal of Machine Learning Research.*, *9*, 1871–1874.

Flynn, K. C. (2013). The cytoskeleton and neurite initiation. *BioArchitecture*, *3*(4), 86–109.

Fries, P. (2015). Rhythms for cognition: Communication through coherence. *Neuron*, *88*(1), 220–235.

Fries, P., Scheeringa, R., & Oostenveld, R. (2008). Finding gamma. *Neuron*, *58*(3), 303–305.

Gaudet, P., Livstone, M. S., Lewis, S. E., & Thomas, P. D. (2011). Phylogenetic-based propagation of functional annotations within the gene ontology consortium. *Briefings in Bioinformatics*, *12*(5), 449–462.

Gotham, K., Risi, S., Pickles, A., & Lord, C. (2007). The autism diagnostic observation schedule: Revised algorithms for improved diagnostic validity. *Journal of Autism and Developmental Disorders*, *37*(4), 613–627.

Gregory, M., & Mandelbaum, D. E. (2012). Evidence of a faster posterior dominant EEG rhythm in children with autism. *Research in Autism Spectrum Disorders*, *6*(3), 1000–1003.

Griesi-Oliveira, K., Suzuki, A. M., Alves, A. Y., Mafra, A., Yamamoto, G. L., Ezquina, S., Magalhães, Y. T., Forti, F. L., Sertie, A. L., Zachi, E. C., Vadasz, E., & Passos-Bueno, M. R. (2018). Actin cytoskeleton dynamics in stem cells from autistic individuals. *Scientific Reports*, *8*(1), 11138.

Hawrylycz, M., Miller, J. A., Menon, V., Feng, D., Dolbeare, T., Guillozet-Bongaarts, A. L., Jegga, A. G., Aronow, B. J., Lee, C. K., Bernard, A., Glasser, M. F., Dierker, D. L., Menche, J., Szafer, A., Collman, F., Grange, P., Berman, K. A., Mihalas, S., Yao, Z., … Lein, E. (2015). Canonical genetic signatures of the adult human brain. *Nature Neuroscience*, *18*(12), 1832–1844.

Herweg, N. A., Solomon, E. A., & Kahana, M. J. (2020). Theta oscillations in human memory. *Trends in Cognitive Sciences*, *24*(3), 208–227.

Hong, S. J., Vos de Wael, R., Bethlehem, R. A. I., Lariviere, S., Paquola, C., Valk, S. L., Milham, M. P., di Martino, A., Margulies, D. S., Smallwood, J., & Bernhardt, B. C. (2019). Atypical functional connectome hierarchy in autism. *Nature Communications*, *10*(1), 1022.

Jurkiewicz, M. T., Gaetz, W. C., Bostan, A. C., & Cheyne, D. (2006). Post-movement beta rebound is generated in motor cortex: Evidence from neuromagnetic recordings. *NeuroImage*, *32*(3), 1281–1289.

Kleinhans, N. M., Richards, T., Sterling, L., Stegbauer, K. C., Mahurin, R., Johnson, L. C., Greenson, J., Dawson, G., & Aylward, E. (2008). Abnormal functional connectivity in autism spectrum disorders during face processing. *Brain*, *131*(Pt 4), 1000–1012.

Klimesch, W. (1999). EEG alpha and theta oscillations reflect cognitive and memory performance: A review and analysis. *Brain Research. Brain Research Reviews*, *29*(2–3), 169–195.

Lee, Y., Park, B. Y., James, O., Kim, S. G., & Park, H. (2017). Autism spectrum disorder related functional connectivity changes in the language network in children adolescents and adults. *Frontiers in Human Neuroscience*, *11*, 418.

Li, J., Seidlitz, J., Suckling, J., Fan, F., Ji, G. J., Meng, Y., Yang, S., Wang, K., Qiu, J., Chen, H., & Liao, W. (2021). Cortical structural differences in major depressive disorder correlate with cell type-specific transcriptional signatures. *Nature Communications*, *12*(1), 1647.

Liu, F., Guo, W., Fouche, J. P., Wang, Y., Wang, W., Ding, J., Zeng, L., Qiu, C., Gong, Q., Zhang, W., & Chen, H. (2015). Multivariate classification of social anxiety disorder using whole brain functional connectivity. *Brain Structure & Function*, *220*(1), 101–115.

Long, Z., Duan, X., Mantini, D., & Chen, H. (2016). Alteration of functional connectivity in autism spectrum disorder: Effect of age and anatomical distance. *Scientific Reports*, *6*, 26527.

Maenner, M. J., Shaw, K. A., Baio, J., Washington, A., Patrick, M., DiRienzo, M., Christensen, D. L., Wiggins, L. D., Pettygrove, S., Andrews, J. G., Lopez, M., Hudson, A., Baroud, T., Schwenk, Y., White, T., Rosenberg, C. R., Lee, L. C., Harrington, R. A., Huston, M., … Dietz, P. M. (2020). Prevalence of autism spectrum disorder among children aged 8 years - autism and developmental disabilities monitoring network, 11 sites, United States, 2016. *MMWR Surveillance Summaries*, *69*(4), 1–12.

Menon, B. (2019). Towards a new model of understanding - the triple network, psychopathology and the structure of the mind. *Medical Hypotheses*, *133*, 109385.

Menon, V. (2011). Large-scale brain networks and psychopathology: A unifying triple network model. *Trends in Cognitive Sciences*, *15*(10), 483–506.

Nelson, S. B., & Valakh, V. (2015). Excitatory/inhibitory balance and circuit homeostasis in autism spectrum disorders. *Neuron*, *87*(4), 684–698.

Ozonoff, S., Macari, S., Young, G. S., Goldring, S., Thompson, M., & Rogers, S. J. (2008). Atypical object exploration at 12 months of age is associated with autism in a prospective sample. *Autism*, *12*(5), 457–472.

Pang, Y., Zhao, S., Li, Z., Li, N., Yu, J., Zhang, R., Lu, F., Chen, H., Wu, F., Zheng, W., Gao, J., Yang, Y., Wu, H., & Wang, J. (2022). Enduring effect of abuse: Childhood maltreatment links to altered theory of mind network among adults. *Human Brain Mapping*, *43*(7), 2276–2288.

Pereira, F., Mitchell, T., & Botvinick, M. (2009). Machine learning classifiers and fMRI: A tutorial overview. *NeuroImage*, *45*(1 Suppl), S199–S209.

Perez Velazquez, J. L., Barcelo, F., Hung, Y., Leshchenko, Y., Nenadovic, V., Belkas, J., Raghavan, V., Brian, J., & Garcia Dominguez, L. (2009). Decreased brain coordinated activity in autism spectrum disorders during executive tasks: Reduced long-range synchronization in the fronto-parietal networks. *International Journal of Psychophysiology*, *73*(3), 341–349.

Power, J. D., Barnes, K. A., Snyder, A. Z., Schlaggar, B. L., & Petersen, S. E. (2012). Spurious but systematic correlations in functional connectivity MRI networks arise from subject motion. *NeuroImage*, *59*(3), 2142–2154.

Raatikainen, V., Korhonen, V., Borchardt, V., Huotari, N., Helakari, H., Kananen, J., Raitamaa, L., Joskitt, L., Loukusa, S., Hurtig, T., Ebeling, H., Uddin, L. Q., & Kiviniemi, V. (2020). Dynamic lag analysis reveals atypical brain information flow in autism spectrum disorder. *Autism Research*, *13*(2), 244–258.

Romero-Garcia, R., Warrier, V., Bullmore, E. T., Baron-Cohen, S., & Bethlehem, R. A. I. (2019). Synaptic and transcriptionally downregulated genes are associated with cortical thickness differences in autism. *Molecular Psychiatry*, *24*(7), 1053–1064.

Rosen, M. L., Sheridan, M. A., Sambrook, K. A., Dennison, M. J., Jenness, J. L., Askren, M. K., Meltzoff, A. N., & McLaughlin, K. A. (2018). Salience network response to changes in emotional expressions of others is heightened during early adolescence: Relevance for social functioning. *Developmental Science*, *21*(3), e12571.

Sadaghiani, S., & D'Esposito, M. (2015). Functional characterization of the cingulo-opercular network in the maintenance of tonic alertness. *Cerebral Cortex*, *25*(9), 2763–2773.

Salvador, R., Martínez, A., Pomarol-Clotet, E., Gomar, J., Vila, F., Sarró, S., Capdevila, A., & Bullmore, E. (2008). A simple view of the brain through a frequency-specific functional connectivity measure. *NeuroImage*, *39*(1), 279–289.

Sarafoleanu, C., Mella, C., Georgescu, M., & Perederco, C. (2009). The importance of the olfactory sense in the human behavior and evolution. *Journal of Medicine and Life*, *2*(2), 196–198.

Schuch, J. B., Paixão-Côrtes, V. R., Longo, D., Roman, T., Riesgo, R. D. S., Ranzan, J., Becker, M. M., Riegel, M., & Schuler-Faccini, L. (2019). Analysis of a protein network related to copy number variations in autism Spectrum disorder. *Journal of Molecular Neuroscience*, *69*(1), 140–149.

St Pourcain, B., Skuse, D. H., Mandy, W. P., Wang, K., Hakonarson, H., Timpson, N. J., Evans, D. M., Kemp, J. P., Ring, S. M., McArdle, W. L., Golding, J., & Smith, G. D. (2014). Variability in the common genetic architecture of social-communication spectrum phenotypes during childhood and adolescence. *Molecular Autism*, *5*(1), 18.

Stampanoni Bassi, M., Iezzi, E., Gilio, L., Centonze, D., & Buttari, F. (2019). Synaptic plasticity shapes brain connectivity: Implications for network topology. *International Journal of Molecular Sciences*, *20*(24), 6193.

Vitureira, N., Letellier, M., & Goda, Y. (2012). Homeostatic synaptic plasticity: From single synapses to neural circuits. *Current Opinion in Neurobiology*, *22*(3), 516–521.

Walsh, M. J. M., Baxter, L. C., Smith, C. J., & Braden, B. B. (2019). Age group differences in executive network functional connectivity and relationships with social behavior in men with autism Spectrum disorder. *Research in Autism Spectrum Disorder*, *63*, 63–77.

Wu, C. W., Gu, H., Lu, H., Stein, E. A., Chen, J. H., & Yang, Y. (2008). Frequency specificity of functional connectivity in brain networks. *NeuroImage*, *42*(3), 1047–1055.

Yan, Z., Kim, E., Datta, D., Lewis, D. A., & Soderling, S. H. (2016). Synaptic actin dysregulation, a convergent mechanism of mental disorders? *The Journal of Neuroscience*, *36*(45), 11411–11417.

Yerys, B. E., Gordon, E. M., Abrams, D. N., Satterthwaite, T. D., Weinblatt, R., Jankowski, K. F., Strang, J., Kenworthy, L., Gaillard, W. D., & Vaidya, C. J. (2015). Default mode network segregation and social deficits in autism spectrum disorder: Evidence from non-medicated children. *Neuroimage Clinical*, *9*, 223–232.

SUPPORTING INFORMATION

Additional supporting information can be found online in the Supporting Information section at the end of this article.

How to cite this article: Long, J., Lu, F., Yang, S., Zhang, Q., Chen, X., Pang, Y., Wang, M., He, B., Liu, H., Duan, X., Chen, H., Ye, S., & Chen, H. (2023). Different functional connectivity optimal frequency in autism compared with healthy controls and the relationship with social communication deficits: Evidence from gene expression and behavior symptom analyses. *Human Brain Mapping*, *44*(1), 258–268. https://doi.org/10.1002/hbm.26011